ANTICANCER RESEARCH *40*: 3355-3360 (2020)
doi:10.21873/anticanres.14318

Classification Model to Estimate MIB-1 (Ki 67) Proliferation Index in NSCLC Patients Evaluated With ^{18}F-FDG-PET/CT

BARBARA PALUMBO[1], ROSANNA CAPOZZI[2], FRANCESCO BIANCONI[3], MARIO LUCA FRAVOLINI[3], SILVIA CASCIANELLI[3], SALVATORE GERARDO MESSINA[4], GUIDO BELLEZZA[5], ANGELO SIDONI[5], FRANCESCO PUMA[2] and MARK RAGUSA[6]

[1]*Section of Nuclear Medicine and Health Physics, Department of Surgical and Biomedical Sciences, Università degli Studi di Perugia, Perugia, Italy;*
[2]*Section of Thoracic Surgery, Università degli Studi di Perugia, Azienda Ospedaliera "S. Maria della Misericordia", Perugia, Italy;*
[3]*Department of Engineering, Università degli Studi di Perugia, Perugia, Italy;*
[4]*Nuclear Medicine Division, Azienda Ospedaliera di Perugia, Perugia, Italy;*
[5]*Section of Anatomic Pathology and Histology, Department of Experimental Medicine, Università degli Studi di Perugia, Perugia, Italy;*
[6]*Thoracic Surgery Unit, Azienda Ospedaliera "S. Maria", Terni, Italy*

Abstract. *Background/Aim: Proliferation biomarkers such as MIB-1 are strong predictors of clinical outcome and response to therapy in patients with non-small-cell lung cancer, but they require histological examination. In this work, we present a classification model to predict MIB-1 expression based on clinical parameters from positron emission tomography. Patients and Methods: We retrospectively evaluated 78 patients with histology-proven non-small-cell lung cancer (NSCLC) who underwent ^{18}F-FDG-PET/CT for clinical examination. We stratified the population into a low and high proliferation group using MIB-1=25% as cut-off value. We built a predictive model based on binary classification trees to estimate the group label from the maximum standardized uptake value (SUV_{max}) and lesion diameter. Results: The proposed model showed ability to predict the correct proliferation group with overall accuracy >82% (78% and 86% for the low- and high-proliferation group, respectively). Conclusion: Our results indicate that radiotracer activity evaluated via SUV_{max} and lesion diameter are correlated with tumour proliferation index MIB-1.*

Lung cancer is currently estimated as the first and third most common form of cancer in men and women worldwide, respectively (1). In the United States, lung & bronchus cancer is by far the leading cause of cancer-related deaths in both genders, accounting for ~24% of all cancer-related casualties [2019 estimates (2)]. Histologically, NSCLC is the most common variation, with an estimated relative incidence of ~83% (3). Tobacco smoking is the major risk factor for lung cancer, but other elements such as genetics, chronic inflammation, occupational exposure, air pollution and poor diet have also been investigated as potential determinants (4). Despite the steady (but slow) increase experienced during the last 40 years, the average five-year survival rate for NSCLC is still rather appalling [~25% (3)]. Timely detection and personalised care are currently considered as key factors for improving the clinical outcome of patients affected by this disease (5).

Fluorine 18 (^{18}F) fluorodeoxyglucose positron emission tomography/computed tomography (PET/CT in the remainder) plays a major role in a number of tasks related to the management of patients with NSCLC such as staging, re-staging, detection of recurrence and evaluation of response to therapy (6-8). PET/CT has also proved useful in screening programmes for detecting lung cancer at an early stage (9). Standardized uptake value (SUV) is a semi-quantitative parameter representing the ratio between the activity in the tissue and the whole injected dose relative to body weight. The maximum value of SUV (SUV_{max} henceforth) is possibly the most commonly used PET-derived parameter in oncological clinical practice (7, 10). High values of SUV_{max} are considered as predictors of higher risk of recurrence and generally worse prognosis in patients with NSCLC (11-14). Likewise, SUV_{max} has been reported to be useful for

Correspondence to: Francesco Bianconi, Department of Engineering, Via Goffredo Duranti 93, 06125 Perugia, Italy. Tel: +39 0755859738, e-mail: bianco@ieee.org

Key Words: ^{18}F-FDG PET/CT, non-small-cell lung cancer, MIB-1, artificial intelligence.

discriminating between malignant and benign lung nodules, mainly as a consequence of the higher values exhibited by malignant lesions compared with benign ones (10, 15, 16). A moderate positive correlation between SUV_{max} and tumour size in patients with NSCLC has also been reported (17), thus implicitly confirming the correlation between SUV_{max} and tumour aggressiveness. In some studies, the ratio between SUV_{max} and primary tumour size has been reported as a more important indicator of prognosis than SUV_{max} alone (18, 19).

Proliferation biomarkers such as MIB-1 have long been recognised as strong predictors of clinical outcome and response to therapy in patients with NSCLC (20- 22). Since tumours showing higher SUV_{max} are also considered more aggressive and highly proliferative, much research in recent years has focussed on the potential correlations between SUV_{max} and proliferation activity markers. Among them, the relationship between the Ki-67 expression index and the degree of radiotracer uptake in NSCLC evaluated through SUV_{max} has been investigated in several studies (10, 23, 24). High SUV_{max} is also considered as an independent predictor of programmed cell death ligand 1 (PD-L1) expression (25). Direct analysis of molecular biomarkers, however, is only possible after biopsy and/or surgical resection of the lesion, none of which options is always a viable approach in clinical practice. Therefore, there is much interest in determining whether it is possible to estimate tumour proliferation markers from radiomic data. In this study we present an approach for estimating MIB-1 on primary lesions in patients with NSCLC using PET/CT data – specifically SUV_{max} and lesion diameter. The method is based on classification trees (ClT in the remainder), an artificial intelligence technique which enables automatic classification through a set of logical rules defined as binary options on sets of discriminative cut-off values of the input parameters.

Patients and Methods

Patient population. We retrospectively evaluated 78 patients with histology-proven NSCLC who were referred for PET/CT examination and treated at the Thoracic Surgery Unit of the Perugia University Medical School (Hospital 'S. Maria della Misericordia', Perugia, Italy). The clinical characteristics of the patient series are detailed in Table I. All patients gave written informed consent to undergo PET/CT for clinical purposes and to accept that their data could be used in anonymous form for scientific studies.

Examination protocol. PET/CT examination was carried out on a hybrid PET/CT scanner (Discovery ST integrated PET/CTMS system, General Electric Medical Systems, Waukesha, WI, USA) consisting of a combination of a four-detector row (912 detectors per row) CT unit and one PET scanner with bismuth germanate crystals in 24 rings. The patients were fasted for at least 12h before the scan and serum glucose levels were measured to confirm values below 120mg/dL (6.66 mmol/l). Weight and height of all the patients were also recorded. Fluorine 18 fluorodeoxyglucose was administered intravenously to each patient in a single bolus (340-450 MBq) 45-60 min before the PET scan, followed by 250-500 ml of saline solution. Subsequently, the patients were invited to stretch out within the gantry in a supine position with their arms raised to decrease beam-hardening artifacts. Unenhanced low-dose (80 mA) CT was carried out for attenuation correction with the following parameters: section thickness 3.75 mm; reconstruction index 1.25 mm; gantry rotation speed <1 s; pitch, 1-1.5 and tube voltage 140 kVp. For a more faithful reproduction of the anatomic conditions the entire CT volume was obtained during one single breath hold. After unenhanced computed-tomography, PET examination was performed with a two-dimensional technique in caudo-cranial direction from the proximal one-third of the femour to the skull and the duration of each scan was approximately 4 min. The other parameters were: matrix size 128px × 128px, zoom factor 1 and full-width at half maximum 4.69. The images were reconstructed by using axial-, coronal-, and sagittal-plane views and were corrected for attenuation through the CT data by ordered subsets expectation maximization algorithm. The average PET examination time was 24-28 min.

Table I. *Characteristics of the patient series*.

Demographics	
Age [median (range), yrs]	69 (51-84)
Male [N (%)]	64 (82.1%)
Female [N (%)]	14 (17.9%)
Histology	
Adenocarcinoma [N (%)]	45 (57.7%)
Squamous cell carcinoma [N (%)]	26 (33.3%)
Other [N (%)]	7 (9%)
Surgery	
Pneumonectomy [N (%)]	6 (7.7%)
Bilobectomy [N (%)]	3 (3.8%)
Lobectomy [N (%)]	65 (83.3%)
Segmentectomy [N (%)]	3 (3.8%)
R1 resection margin [N (%)]	1 (1.3%)
Grade	
Well differentiated [N (%)]	9 (11.5%)
Moderately differentiated [N (%)]	42 (53.8%)
Scarcely differentiated [N (%)]	27 (34.6%)
Stage	
IA/IB [N (%)]	47 (60.2%)
IIA/IIB [N (%)]	16 (20.5%)
IIIA [N (%)]	15(19.2%)

The resulting PET/CT scans were read independently by two nuclear medicine specialists (B.P. and S.G.M. – both with >15 yrs experience). SUV_{max} values were obtained by drawing the regions of interest over the most intense slice of the primary after correcting for the injected dose and the patient's weight (19). The tumour diameter in the primary site was also measured.

Immunohistochemistry. Immunohistochemistry (IHC) was performed on 4 μm formalin-fixed paraffin-embedded (FFPE) sections from the most representative area of each lesion using a monoclonal antibody targeting Ki67 (Clone Mib1, DAKO, dilution 1:100). The signal was detected using a biotin-free polymeric-

Table II. *Overall and per-class accuracy.*

Model	Accuracy (mean %)		
	Overall	Class 'A'	Class 'B'
SUV_{max} + lesion diameter	82.05%	78.05%	86.49%
SUV_{max}	79.49%	92.68%	64.86%
Lesion diameter	65.38%	70.73%	59.46%

Table III. *Parameter values (whole population and by class).*

Parameter	Value (mean±std. dev.)		
	All subjects	Class 'A'	Class 'B'
MIB-1	25.23 (±15.11)	13.12 (±4.23)	38.65 (±10.39)
SUV_{max}	9.34 (±5.82)	6.89 (±4.24)	12.06 (±6.17)
Lesion diameter	27.19 (±14.78)	22.78 (±0.00)	32.08 (±18.70)

horseradish peroxidase (HRP)- linker antibody conjugate system (Bond Polymer Refine Detection, Leica BioSystems, Newcastle, UK) with heat-induced epitope retrieval (pH 6 for 30 min). The slides were stained using the Bond III automated immunostainer (Leica BioSystems Pty Ltd., Melbourne, Australia) and semi-quantitative evaluation of the staining was performed. Only nuclear staining of the tumour cells was scored. The results were expressed as the fraction (in percentage) between the number of positive nuclei and the total number of nuclei examined.

Standard of reference. The standard of reference for diagnosis of all lesions was histological examination and clinical results and findings of follow-up imaging [conventional CT and/or magnetic resonance (MR) imaging and/or ultrasonography (US)] for at least 6 months. The evaluation of the clinical records and the clinical follow-up of the patients were performed and discussed in consensus at the multidisciplinary meetings of our hospital, and no conflicting results emerged.

Classification trees. Classification trees (also referred to as decision trees) are a type of classifier that reaches the decision through a set of questions applied individually to each feature of the input pattern. In this work we used binary classification trees, which are based on questions of the kind 'is $f_i \leq t_i$?', being f_i the i-th feature and t_i the decision value (also referred to as threshold) for that feature (26).

The set of questions and the corresponding thresholds are determined by training, which is carried out on a set of pre-classified cases (train set). The training process involves the following steps: a) defining a splitting criterion to divide the data into two subsets while maximising the intra-subset homogeneity; b) at each node deciding the candidate questions to be asked; c) establishing a stop-splitting rule to control the growth of the tree and d) establishing a rule to assign each leaf to one of the possible classes. Further refinement of the tree can be obtained by pruning, which consists of removing the levels (decision rules) that are irrelevant for the classification. At the end of the training process the ClT will consist of a set of logical rules which can be used to make predictions about the clinical conditions of the patient under evaluation.

Classification trees are particularly appealing in that they are fast, relatively easy to train and able to provide performance similar to that obtainable *via* more sophisticated methods. Furthermore, the inference mechanism of ClT [the 'gathered knowledge' (27)] is – unlike other methods – human-readable, and, as such, can be encoded into rules than can be easily translated into clinical practice.

Estimation of MIB-1 expression. We used classification trees to estimate MIB-1 from SUV_{max} and lesion diameter. To this end we evaluated three different ClT structures based on the following combinations of the input features: 1) SUV_{max} and lesion diameter; 2) SUV_{max} only and 3) lesion diameter only. For each of the above combinations we tested ClTs with different degree of complexity, the latter being determined by the amount of pruning on the original ClT.

Experiments. We cast the MIB-1 estimation process into a binary classification problem in the following way: cases with MIB-1 ≤25% were labelled as class 'A', the others (MIb-1 >25%) as class 'B'. Accuracy estimation was based on leave-one-out cross-validation (26) – *i.e.* each classification model was trained using the data of all the patients but one and tested on the left-out case. The overall accuracy was the average of the results obtained over all the subdivisions into train and test set. The implementation was based on Matlab's Neural Networks Toolbox (28).

Results

Table II summarises the classification results. As can be seen, the best overall performance was achieved by using both SUV_{max} and lesion diameter as input features, which gave 82.05% overall accuracy (per-class accuracy 78.05% and 86.49% for 'A' and 'B', respectively). The models that used only one of the two features had worse performance: SUV_{max} alone achieved 79.49% overall accuracy (92.68% and 64.86% for class '1' and '2', respectively); lesion diameter alone provided 65.38% (70.73% and 59.46%).

Table III reports the mean values and standard deviation of MIB-1, SUV_{max} and lesion diameter in the patient population. Looking at the structure of the ClT that achieved the best accuracy (Figure 1), we can see that a) SUV_{max} below 3.95 alone was indicative of low proliferation index (MIB-1 ≤25%); b), lesion diameter above 41.5mm alone or below that threshold but with SUV_{max} ≥17.8 was indicative of high proliferation index (MIB-1 >25%) and c) lesion diameter below 41.5mm and SUV_{max} in the range 6.6-17.8 indicated low proliferation index.

Discussion

Tumour proliferation biomarkers play a pivotal role in predicting the overall outcome and response to treatment in patients with NSCLC. However, the determination of such

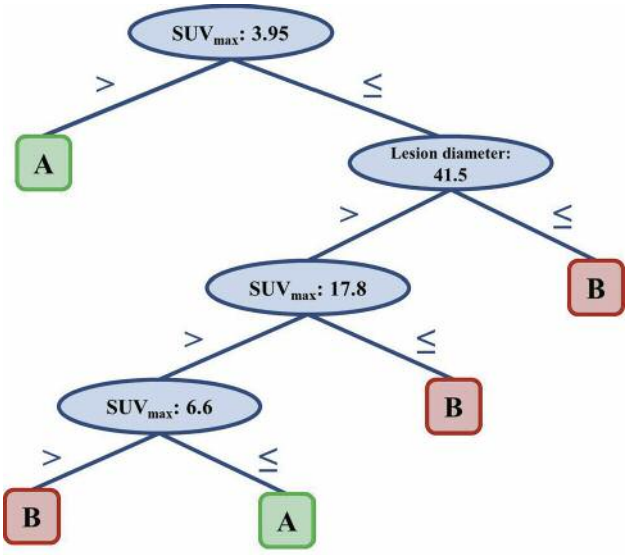

Figure 1. *Structure of the classification tree in the population studied.*

biomarkers is only possible after tissue biopsy and/or surgical resection, none of which options is free of risk and always necessarily requested in clinical practice. The possibility to estimate such data non-invasively can be of great help in the process of lesion characterisation.

Many authors have set into evidence the relationship between pathological type of NSCLC, lesion size and SUV_{max} as measured by PET/CT (29-31). Özgül *et al.* (29) for instance have found that SUV_{max} was significantly associated with tumour size. Specifically, they divided patients with NSCLC in three groups, according to tumor size (group 1, ≤3 cm; group 2, between 3 cm and 5 cm; group 3, >5 cm) and showed that SUV_{max} was significantly lower in groups 1 and 2 compared with group 3. Hsu *et al.* (30) have shown that patients with a reference lung tumor ≤3 cm and SUV ≤3.1 had an expected five-year survival of 100%, while subjects with a reference tumour >3 cm and SUV >3.1 had an expected five-year survival rate of 53.3%. Karam *et al.* (31) have reported a significant correlation between SUV_{max}, tumour differentiation and tumour size in patients with adenocarcinoma and between SUV_{max} and tumour size of individuals with squamous cell carcinoma. The authors also concluded that the overall SUV_{max} of patients with NSCLC could be predicted by tumour size value, the prediction being more accurate for patients with adenocarcinoma compared with those with squamous cell carcinoma.

In this work we investigated the correlation between the proliferation biomarker MIB-1 (Ki 67) and radiomic data – specifically SUV_{max} and lesion diameter from PET/CT. With this aim we split the patient population into a low and a high proliferation group using MIB-1=25% as threshold, then trained an automatic classifier to determine whether an unknown case could be correctly classified as low or high group based on SUV_{max} and lesion diameter from PET/CT. Our method could correctly predict the class label with overall accuracy >82% by using both radiomic parameters (SUV_{max} and lesion diameter) as input features. The results indicate that radiotracer activity evaluated *via* SUV_{max} and lesion diameter is correlated with the tumour proliferation index MIB-1. This is of clinical interest as the tumour proliferation marker MIB-1 reflects biological aggression. Furthermore, the use of an artificial intelligence technique like ClT enables the classification model to be encoded into a set of rules easily interpreted by humans.

This work is not exempt from limitations. Among them are its retrospective nature and the relatively limited sample size (n=78). The results found here are encouraging and should be validated in larger studies. Interesting directions for future work include the investigation of other radiomic parameters (*e.g.* shape and texture features from PET/CT) and their potential correlation with tumour proliferation index.

Conflicts of Interest

The Authors declare no conflicts of interest regarding this study.

Authors' Contributions

Conceptualization: B.P., F.P. and M.R.; Data collection and preparation: B.P., R.C. and S.C., S.G.M., G.B. and M.R.; Mathematical modelling and data analysis: M.L.F., S.C., and F.B.; Validation: B.P., R.C., M.L.F., G.B., S.G.M., A.S. and M.R.; Supervision, B.P., F.B., M.L.F., A.S., F.P and M.R.; Writing – preparation of the original draft, B.P., F.B., M.L.F., G.B. and M.R.; Writing – review and editing: all authors; Funding acquisition, B.P. and F.B. All Authors have read and agreed to the submitted version of the manuscript.

Acknowledgements

This work was partially supported by the Fondazione Cassa di Risparmio di Perugia (Perugia, Italy), under grant no. 2015.0389013 – "Application of Artificial Intelligence methods to PET/CT for computer-assisted diagnosis", and by the Department of Engineering, Università degli Studi di Perugia (Perugia, Italy) under project "Shape, colour and texture features for the analysis of two- and three-dimensional images: methods and applications" (Fundamental Research Grants Scheme 2019).

References

1 American Institute for Cancer Research. Lung cancer statistics. lung cancer is the most common cancer worldwide. Available at: https://www.wcrf.org/dietandcancer/cancer-trends/lung-cancer-statistics [Last accessed on 23 Dec, 2019]

2 Siegel R, Miller K and Jemal A: Cancer statistics, 2019. CA Cancer J Clin *69(1)*: 7-34, 2019. PMID: 30620402. DOI: 10.3322/caac.21551
3 Howlader N, Noone A, Krapcho M, Miller D, Brest A, Yu M, Ruhl J, Tatalovich Z, Mariotto A, Lewis D, Chen H, Feuer EJ and Cronin S: Seer cancer statistics review, 1975-2016. National Cancer Institute. Bethesda, MD, USA. Available at: https://seer.cancer.gov/csr/1975_2016/, based on November 2018 SEER data submission, posted to the SEER web site, April 2019. [Last accessed on 23 Dec, 2019]
4 Malhotra J, Malvezzi M, Negri E, La Vecchia C and Boffetta P: Risk factors for lung cancer worldwide. Eur Respir J *48(3)*: 889-902, 2016. PMID: 27174888. DOI: 10.1183/13993003.00359-2016
5 Mascaux C, Tomasini P, Greillier L and Barlesi F: Personalised medicine for nonsmall cell lung cancer. Eur Respir Rev *26(146)*: 170066, 2017. PMID: 29141962. DOI: 10.1183/16000617.0066-2017
6 Aristei C, Falcinelli L, Palumbo B and Tarducci R: PET and PET-CT in radiation treatment planning for lung cancer. Expert Rev Anticancer Ther *10(4)*: 571-584, 2010. PMID: 20397922. DOI: 10.1586/era.09.195
7 Liu J, Dong M, Sun X, Li W, Xing L and Yu J: Prognostic value of ^{18}F-FDG PET/CT in surgical non-small cell lung cancer: A meta-analysis. PLoS One *11(1)*: e0146195, 2016. PMID: 26727114. DOI: 10.1371/journal.pone.0146195
8 Greenspan B: Role of PET/CT for precision medicine in lung cancer: perspective of the Society of Nuclear Medicine and Molecular Imaging. Transl Lung Cancer Res *6(6)*: 617-620, 2017. PMID: 29218264. DOI: 10.21037/tlcr.2017.09.01
9 Minamimoto R, Senda M, Jinnouchi S, Terauchi T, Yoshida T, Uno K, Iinuma T, Murano T, Nakashima R and Inoue T: Detection of lung cancer by FDG-PET cancer screening program: A nationwide Japanese survey. Anticancer Res *34(1)*: 183-189, 2014. PMID: 24403460.
10 Shimizu K, Maeda A, Yukawa T, Nojima Y, Saisho S and Nakata R: Difference in prognostic values of maximal standardized uptake value on fluorodeoxyglucose positron emission tomography and cyclooxygenase-2 expression between lung adenocarcinoma and squamous cell carcinoma. World J Surg Oncol *12(1)*, 2014. PMID: 25392182. DOI: 10.1186/1477-7819-12-343
11 Liu J, Dong M, Sun X, Li W, Xing L and Yu J: Prognostic value of ^{18}F-FDG PET/CT in surgical non-small cell lung cancer: A meta-analysis. PLoS One *11(1)*, 2016. PMID: 26727114. DOI: 10.1371/journal.pone.0146195
12 Shirai K, Abe T, Saitoh J, Mizukami T, Irie D, Takakusagi Y, Shiba S, Okano N, Ebara T, Ohno T and Nakano T: Maximum standardized uptake value on FDG-PET predicts survival in stage I non-small cell lung cancer following carbon ion radiotherapy. Oncol Lett *13(6)*: 4420-4426, 2017. PMID: 28588712. DOI: 10.3892/ol.2017.5952
13 Zhu D, Wang Y, Wang L, Chen J, Byanju S, Zhang H and Liao M: Prognostic value of the maximum standardized uptake value of pre-treatment primary lesions in small-cell lung cancer on ^{18}F-FDG PET/CT: a meta-analysis. Acta Radiol *59(9)*: 1082-1090, 2018. PMID: 29256260. DOI: 10.1177/0284185117745907
14 Verma S, Chan J, Chew C and Schultz C: PET-SUV max and upstaging of lung cancer. Heart Lung Circ *28(3)*: 436-442, 2019. PMID: 29428202. DOI: 10.1016/j.hlc.2017.12.011
15 López O, Vicente A, Martínez A, Londoño GAJ, Caicedo CHV, Atance P and Castrejón A: ^{18}F-FDG-PET/CT in the assessment of pulmonary solitary nodules: Comparison of different analysis methods and risk variables in the prediction of malignancy. Transl Lung Cancer Res *4(3)*: 228-235, 2015. PMID: 26207210. DOI: 10.3978/j.issn.2218-6751.2015.05.07
16 Taralli S, Scolozzi V, Foti M, Ricciardi S, Forcione A, Cardillo G and Calcagni M: ^{18}F-FDG PET/CT diagnostic performance in solitary and multiple pulmonary nodules detected in patients with previous cancer history: reports of 182 nodules. Eur J Nucl Med Mol Imaging *46(2)*: 429-436, 2019. PMID: 30535767. DOI: 10.1007/s00259-018-4226-6
17 Bianconi F, Palumbo I, Fravolini M, Chiari R, Minestrini M, Brunese L and Palumbo B: Texture analysis on (^{18}F)FDG PET/CT in non-small-cell lung cancer: Correlations between PET features, CT features, and histological types. Mol Imaging Biol *21(6)*: 1200-1209, 2019. PMID: 30847822. DOI: 10.1007/s11307-019-01336-3
18 Stiles B, Nasar A, Mirza F, Paul S, Lee P, Port J, McGraw T and Altorki N: Ratio of positron emission tomography uptake to tumor size in surgically resected non-small cell lung cancer. Ann Thorac Surg *95(2)*: 397-404, 2013. PMID: 23000262. DOI: 10.1016/j.athoracsur.2012.07.038
19 Chen F, Yao Y, Ma C, Ma X, Wang Z, Lv T, Xiao X, Yin J and Song Y: Ratio of maximum standardized uptake value to primary tumor size is a prognostic factor in patients with advanced non-small cell lung cancer. Transl Lung Cancer Res *4(1)*: 18-26, 2015. PMID: 25806343. DOI: 10.3978/j.issn.2218-6751.2014.11.02
20 Martin B, Paesmans M, Mascaux C, Berghmans T, Lothaire P, Meert AP, Lafitte JJ and Sculier JP: Ki-67 expression and patients survival in lung cancer: Systematic review of the literature with meta-analysis. Br J Cancer *91(12)*: 2018-2025, 2004. PMID: 15545971. DOI: 10.1038/sj.bjc.6602233
21 Yanagawa N, Osakabe M, Ogata S and Shiono S: MIB-1 labeling index is useful as prognostic and predictive markers for adjuvant therapy in non-small cell lung cancer. Ann Oncol *26*: 8-15, 2015. DOI: 10.1093/annonc/mdv518.18
22 Chirieac L: Ki-67 expression in pulmonary tumors. Transl Lung Cancer Res *5(5)*: 547-551, 2016. PMID: 27827465. DOI: 10.21037/tlcr.2016.10.13
23 Deng SM, Zhang W, Zhang B, Chen YY, Li JH and Wu YW: Correlation between the uptake of ^{18}F-fluorodeoxyglucose (^{18}F-FDG) and the expression of proliferation-associated antigen Ki-67 in cancer patients: A meta-analysis. PLoS One *10(6)*, 2015. PMID: 26038827. DOI: 10.1371/journal.pone.0129028
24 Apostolova I, Ego K, Steffen I, Buchert R, Wertzel H, Achenbach H, Riedel S, Schreiber J, Schultz M, Furth C, Derlin T, Amthauer H, Hofheinz F and Kalinski T: The asphericity of the metabolic tumour volume in NSCLC: correlation with histopathology and molecular markers. Eur J Nucl Med Mol Imaging *43(13)*: 2360-2373, 2016. PMID: 27470327. DOI: 10.1007/s00259-016-3452-z
25 Takada K, Toyokawa G, Tagawa T, Kohashi K, Akamine T, Takamori S, Hirai F, Shoji F, Okamoto T, Oda Y and Maehara Y: Association between PD-L1 expression and metabolic activity on ^{18}F-FDG PET/CT in patients with small-sized lung cancer. Anticancer Res *37(12)*: 7073-7082, 2017. PMID: 29187498. DOI: 10.21873/anticanres.12180
26 Theodoridis S and Koutroumbas K: Pattern Recognition. Third edition. Academic Press, Cambridge (MA), United States, 2006.

27 Podgorelec V, Kokol P, Stiglic B and Rozman I: Decision trees: an overview and their use in medicine. J Med Syst *26(5)*: 445-463, 2002. PMID: 12182209. DOI: 10.1023/a:1016409317640

28 Palumbo B, Fravolini M, Nuvoli S, Spanu A, Paulus K, Schillaci O and Madeddu G: Comparison of two neural network classifiers in the differential diagnosis of essential tremor and Parkinson's disease by ^{123}I-FP-CIT brain SPECT. Eur J Nucl Med Mol Imaging *37(11)*: 2146-2153, 2010. PMID: 20567820. DOI: 10.1007/s00259-010-1481-6

29 Özgül M, Kirkil G, Seyhan E, Çetinkaya E, Özgül G and Yüksel M: The maximum standardized FDG uptake on PET-CT in patients with non-small cell lung cancer. Multidiscip Respir Med *8(1)*, 2013. PMID: 24148271. DOI: 10.1186/2049-6958-8-69

30 Hsu CW, Chang CC and Lin CJ: A practical guide to support vector classification. Available at: http://www.csie.ntu.edu.tw/~cjlin/papers/guide/guide.pdf [Last accessed on Mar 22, 2017]

31 Karam M, Doroudinia A, Behzadi B, Mehrian P and Koma A: Correlation of quantified metabolic activity in nonsmall cell lung cancer with tumor size and tumor pathological characteristics. Medicine *97(32)*, 2018. PMID: 30095621. DOI: 10.1097/MD.0000000000011628

Received April 16, 2020
Revised April 30, 2020
Accepted May 4, 2020